stromal cells. J. Orthop. Res. 21, 630-637.

Tenenbaum, L., Lehtonen, E., and Monahan, P.E. (2003). Evaluation of risks related to the use of adeno-associated virus-based vectors. Curr. Gene Ther. 3, 545-565.

Themis, M, Waddington, S.N., Schmidt, M., Von Kalle, C, Wang, Y., Al-Allaf, F, Gregory, L.G., Nivsarkar, M., Holder, M.V., Buckley, S.M., Dighe, N., Ruthe, A.T., Mistry, A., Bigger, B., Rahim, A., Nguyen, T.H., Trono, D., Thrasher, A.J., and Coutelle, C. (2005). Oncogenesis following delivery of a nonprimate lentiviral gene therapy vector to fetal and neonatal mice. Mol. Ther. 12, 763-771.

Waddington, S.N., Buckley, S.M., Nivsarkar, M., Jezzard, S., Schneider, H., Dahse, T., Kemball-Cook, G., Miah, M., Tucker, N., Dallman, M.J., Themis, M., and Coutelle, C. (2003). In utero gene transfer of human factor IX to fetal mice can induce postnatal tolerance of the exogenous clotting factor. Blood 101, 1359-1366.

Watanabe, A., Karasugi, T., Sawai, H., Naing, B.T., Ikegawa, S., Orimo, H., and Shimada, T. (2010). Prevalence of c.1559delT in *ALPL*, a common mutation resulting in the perinatal (lethal) form of hypophosphatasia in Japanese and effects of the mutation on heterozygous carriers. J. Hum. Genet. 56, 166-168.

Whyte, M.P. (2010). Physiological role of alkaline phosphatase explored in hypophosphatasia. Ann N.Y. Acad. Sci. 1192, 190-200.

Yadav, M.C., Lemire, I., Leonard, P., Boileau, G., Blond, L., Beliveau, M., Cory, E., Sah, R.L., Whyte, M.P., Crine, P., and Millán, J.L. (2011). Dose response of bone-targeted enzyme replacement for murine hypophosphatasia. Bone 49, 250–256.

Yamamoto, S., Orimo, H., Matsumoto, T., Iijima, O., Narisawa, S., Maeda, T., Millán, J.L.,

and Shimada, T. (2010). Prolonged survival and phenotypic correction of *Akp2*$^{-/-}$ hypophosphatasia mice by lentiviral gene therapy. J. Bone Miner. Res. 26, 135-142.

Figure legends

Figure 1. Therapeutic effects of fetal gene therapy. (A) Growth curves of *Akp*$^{+/+}$ mice (n = 4, long-dashed lines), untreated *Akp*$^{-/-}$ mice (n = 4, short-dashed lines), and treated *Akp*$^{-/-}$ mice (n = 9, continuous lines). (B) Survival curves of *Akp*$^{+/+}$ mice (n = 8, long-dashed line), untreated *Akp*$^{-/-}$ mice (n = 4, short-dashed line), and treated *Akp*$^{-/-}$ mice (n = 9, continuous line). Statistical analysis revealed that proportion of surviving of treated *Akp*$^{-/-}$ mice was significantly elevated compared to that of untreated *Akp*$^{-/-}$ mice (*$P < 0.001$).

Figure 2. ALP activity in the plasma and tissues. (A) Concentration of plasma ALP activity of *Akp*$^{+/+}$ mice (n = 4, short-dashed line), *Akp*$^{+/-}$ mice (n = 4, long-dashed line), and treated *Akp*$^{-/-}$ mice (n = 3, continuous line) at 14, 28, and 56 days after birth. ALP activity in the plasma of untreated *Akp*$^{-/-}$ mice (n = 4) at 10 days after birth is indicated as a square marker. (B) ALP activity in the tissues of *Akp*$^{+/+}$ mice (day 14; n = 2 – 3, gray bars), untreated *Akp*$^{-/-}$ mice (day 10; n = 3, white bars) and treated *Akp*$^{-/-}$ mice (day 14; n = 3, black bars). Data are presented as means and SD. Student's t test was employed for comparisons between the two groups (*$P < 0.01$, **$P < 0.05$).

Figure 3. Histochemical staining for ALP activity. ALP activity is shown as purple staining. The pictures show the tibial bones of 14-day-old (A) and 56-day-old (B) *Akp*$^{+/+}$ mice, 10-day-old untreated *Akp*$^{-/-}$ mouse (C), 14-day-old (D) and 56-day-old (E) treated *Akp*$^{-/-}$ mice. Bars = 250 μm.

Figure 4. X-ray images. (A) Forepaw of 10-day-old untreated *Akp*$^{-/-}$ mouse, *Akp*$^{+/+}$ mouse, and treated *Akp*$^{-/-}$ mouse. (B) Thoracic cage of 56-day-old *Akp*$^{+/+}$ mouse and treated *Akp*$^{-/-}$ mouse.

Figure 5. Biodistribution of AAV9-EGFP (real-time PCR). (A) Vector copy number in each tissue of *Akp*$^{+/+}$ mice after fetal (n = 3, black bar) or neonatal (n = 3, white bar) IP injection of AAV9-EGFP (real-time PCR). Data are presented as means and SD. Student's t test was employed for comparisons between the two groups (*$P < 0.01$, **$P < 0.05$). (B) DAB staining of tibial bone after fetal IP injection (a, b) and neonatal IP injection (c, d). Negative controls (e, f) were mice without vector injection. (b), (d), and (f) High-resolution photographs of the frames in (a), (c), and (e), respectively. Bars = 250 μm. (C) Immunostaining of tibial bone with anti-GFP (a), anti-collagen type II (b), and the merge of anti-GFP and anti-collagen type II (c). Bars = 50 μm.

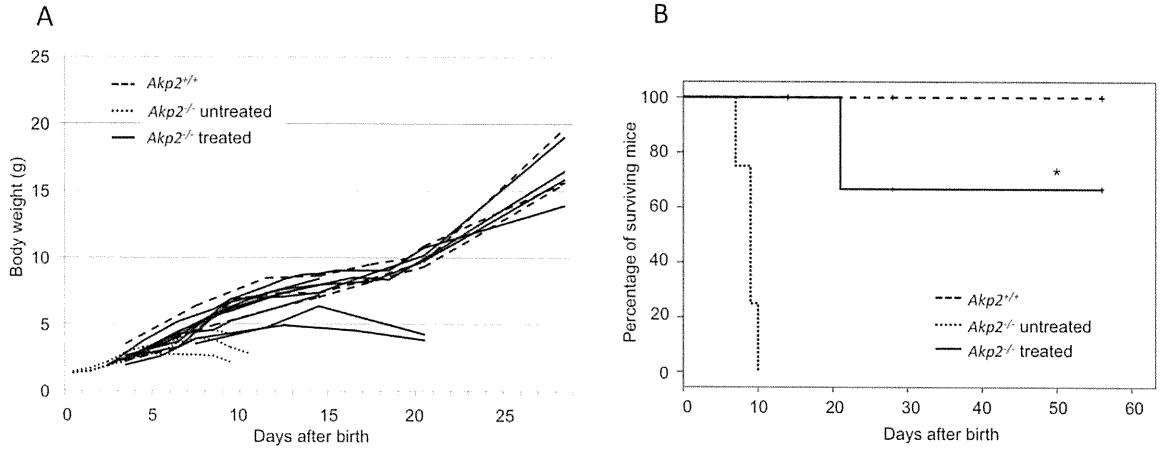

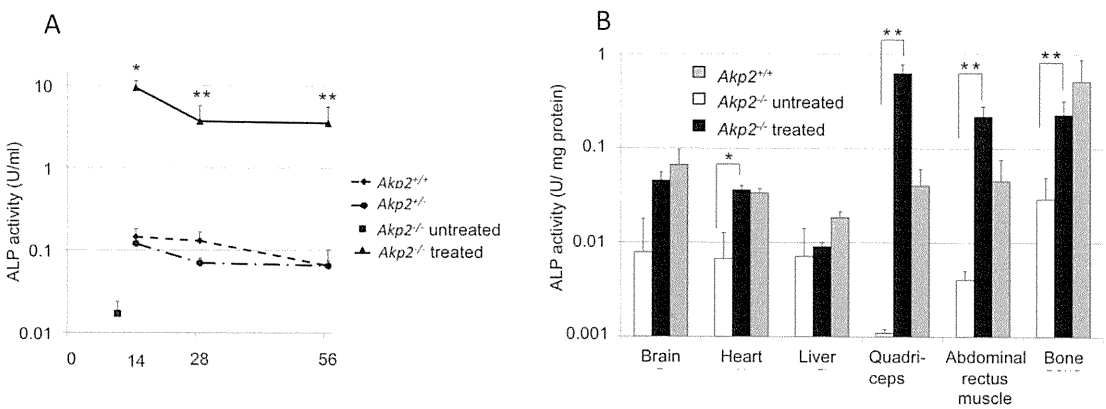

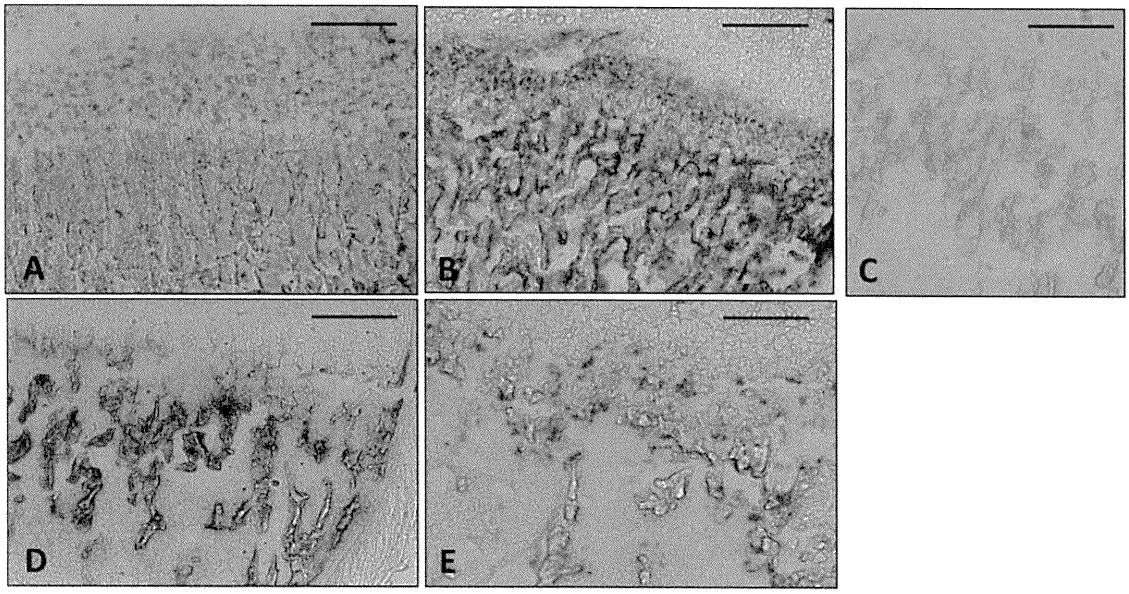

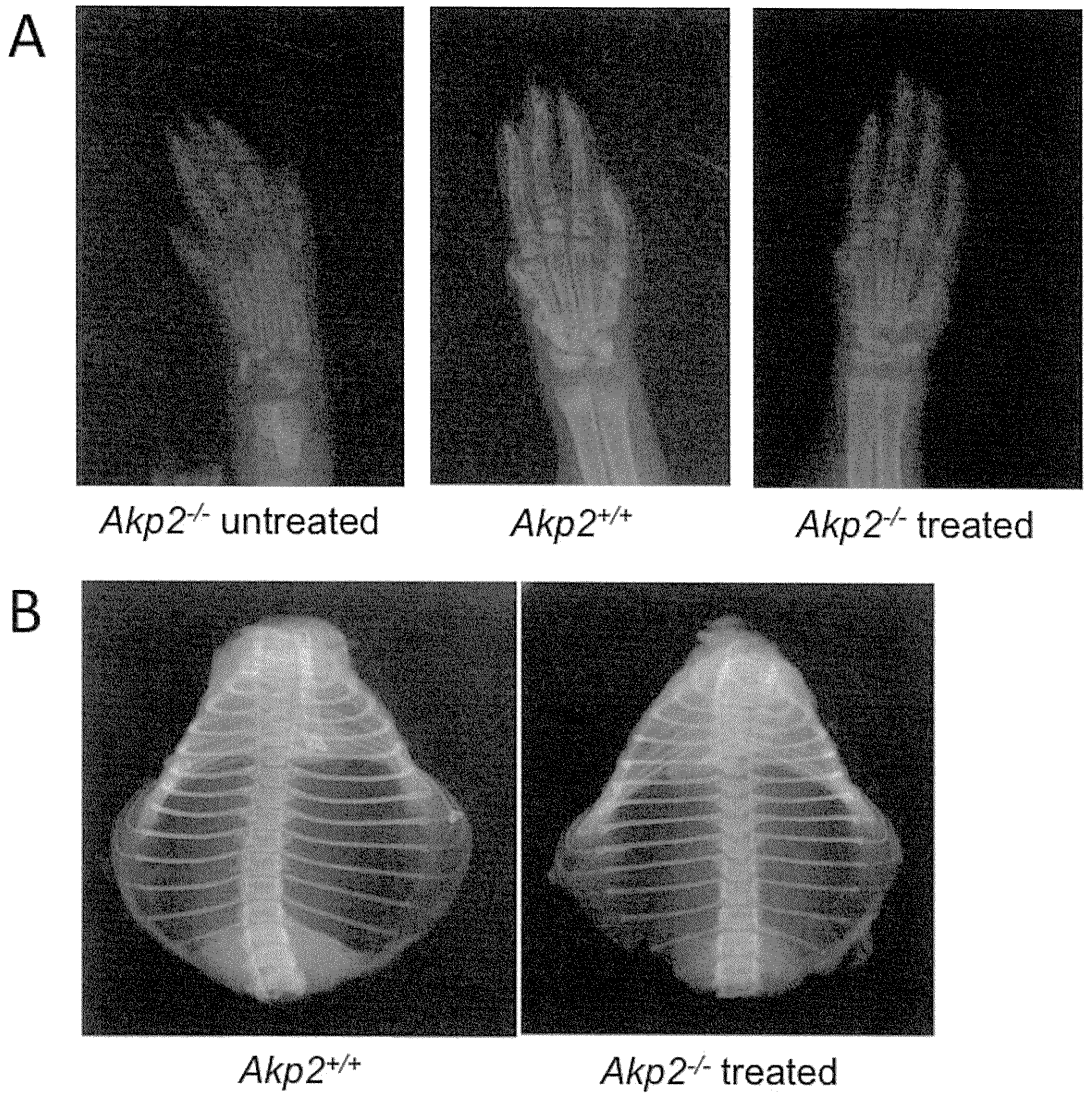

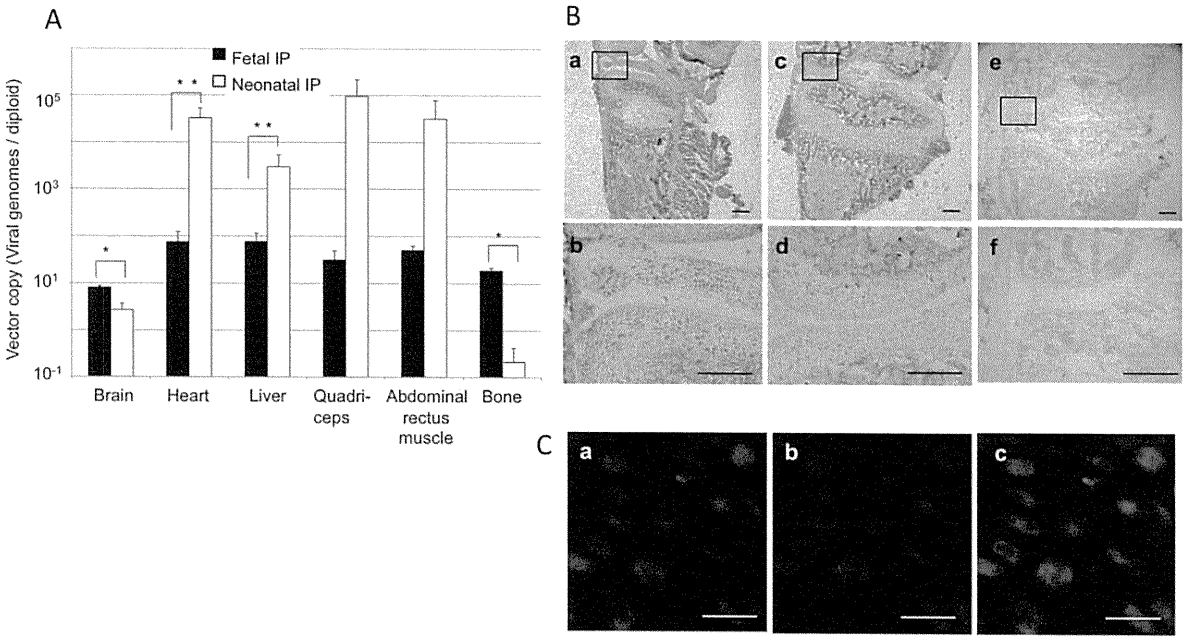

HUMAN GENE THERAPY 22:1355–1364 (November 2011)

DOI: 10.1089/hum.2010.210

Rescue of Severe Infantile Hypophosphatasia Mice by AAV-Mediated Sustained Expression of Soluble Alkaline Phosphatase

Tae Matsumoto,[1,2] Koichi Miyake,[1,3] Seiko Yamamoto,[1,4] Hideo Orimo,[1] Noriko Miyake,[1,3] Yuko Odagaki,[1,3] Kumi Adachi,[1,3] Osamu Iijima,[1,3] Sonoko Narisawa,[4] José Luis Millán,[4] Yoshitaka Fukunaga,[2] and Takashi Shimada[1,3]

Abstract

Hypophosphatasia (HPP) is an inherited disease caused by a deficiency of tissue-nonspecific alkaline phosphatase (TNALP). The major symptom of human HPP is hypomineralization, rickets, or osteomalacia, although the clinical severity is highly variable. The phenotypes of TNALP knockout (*Akp2*$^{-/-}$) mice mimic those of the severe infantile form of HPP. *Akp2*$^{-/-}$ mice appear normal at birth, but they develop growth failure, epileptic seizures, and hypomineralization and die by 20 days of age. Previously, we have shown that the phenotype of *Akp2*$^{-/-}$ mice can be prevented by enzyme replacement of bone-targeted TNALP in which deca-aspartates are linked to the C-terminus of soluble TNALP (TNALP-D10). In the present study, we evaluated the therapeutic effects of adeno-associated virus serotype 8 (AAV8) vectors that express various forms of TNALP, including TNALP-D10, soluble TNALP tagged with the Flag epitopes (TNALP-F), and native glycosylphosphatidylinositol-anchored TNALP (TNALP-N). A single intravenous injection of 5×10^{10} vector genomes of AAV8-TNALP-D10 into *Akp2*$^{-/-}$ mice at day 1 resulted in prolonged survival and phenotypic correction. When AAV8-TNALP-F was injected into neonatal *Akp2*$^{-/-}$ mice, they also survived without epileptic seizures. Interestingly, survival effects were observed in some animals treated with AAV8-TNALP-N. All surviving *Akp2*$^{-/-}$ mice showed a healthy appearance and a normal activity with mature bone mineralization on X-rays. These results suggest that sustained alkaline phosphatase activity in plasma is essential and sufficient for the rescue of *Akp2*$^{-/-}$ mice. AAV8-mediated systemic gene therapy appears to be an effective treatment for the infantile form of human HPP.

Introduction

HYPOPHOSPHATASIA (HPP) is an inherited systemic skeletal disease characterized by a deficiency in tissue-nonspecific alkaline phosphatase (TNALP), which is attached to the outer cell membrane of many cell types via a glycosylphosphatidylinositol (GPI) anchor (Millán, 2006). The major symptom of human HPP is hypomineralization, rickets, or osteomalacia, although the clinical severity is highly variable and ranges from a lethal perinatal form to mild odontohypophosphatasia that manifests only dental abnormalities (Whyte, 2002; Mornet, 2007). Patients with infantile HPP may appear normal at birth, but they gradually develop rickets before 6 months of age. Pyridoxine-responsive seizures often occur in severe forms of infantile HPP (Mornet, 2007).

Several approaches have been tried in an effort to treat patients with HPP. These treatments include transplantation of bone marrow cells (Whyte *et al.*, 2003; Tadokoro *et al.*, 2009), transplantation of bone fragments and cultured osteoblasts (Cahill *et al.*, 2007), the administration of parathyroid hormone (Whyte *et al.*, 2007; Camacho *et al.*, 2008), enzyme replacement therapy (ERT) with alkaline phosphatase (ALP)-rich serum from patients with Paget's disease of the bone (Whyte *et al.*, 1984), and the infusion of plasma from healthy individuals (Whyte *et al.*, 1986) or ALP purified from liver (Weninger *et al.*, 1989). These treatments have provided limited clinical and radiographic improvements in a few patients.

The phenotypes of TNALP knockout (*Akp2*$^{-/-}$) mice mimic those of severe infantile HPP; therefore, these *Akp2*$^{-/-}$ mice

[1]Department of Biochemistry and Molecular Biology, Nippon Medical School, Tokyo 113-8602, Japan.
[2]Department of Pediatrics, Nippon Medical School, Tokyo 113-8603, Japan.
[3]Division of Gene Therapy Research Center for Advanced Medical Technology, Nippon Medical School, Tokyo 113-8602, Japan.
[4]Sanford Children's Health Research Center, Sanford-Burnham Medical Research Institute, La Jolla, CA 92037.

have been used as an animal model for HPP (Narisawa *et al.*, 1997). They appear normal at birth, but they rapidly develop growth failure, epileptic seizures, and hypomineralization and die by 20 days of age. We reported that the phenotype of *Akp2*$^{-/-}$ mice could be corrected by daily subcutaneous injections of a bone-targeted form of TNALP, which is created by linking a bone-targeting deca-aspartate sequence to the C-terminus of soluble TNALP (TNALP-D10) (Millán *et al.*, 2008). Based on these data, new clinical trials of ERT for patients with HPP have been initiated (http://clinicaltrials.gov).

Gene therapy has proven to be a useful tool for the treatment of several inherited diseases. Recently, we demonstrated that a single injection of lentiviral vector expressing TNALP-D10 resulted in sustained expression of TNALP and phenotypic correction of *Akp2*$^{-/-}$ mice (Yamamoto *et al.*, 2011). This gene therapy approach is referred to as viral vector–mediated ERT, and it is more practical than classical ERT, which requires repeated injections. One way to develop this approach is *in vivo* gene therapy with adeno-associated virus (AAV) vector. In the present study, we evaluated AAV vectors expressing various forms of TNALP. We found that AAV-mediated expression of soluble TNALP resulted in prolonged survival and the phenotypic correction of *Akp2*$^{-/-}$ mice.

Materials and Methods

Cell culture

The C2C12, HEK 293, and U2OS (human osteosarcoma HTB-96; ATCC, Manassas, VA) cell lines were cultured in Dulbecco's modified Eagle medium supplemented with 10% fetal bovine serum, 50 U/ml penicillin, and 50 μg/ml streptomycin under an atmosphere enriched with 5% CO_2.

Plasmid construction and vector production

The plasmids containing cDNA for native GPI-anchored TNALP (TNALP-N) (Goseki-Sone *et al.*, 1998), TNALP-D10 (Yamamoto *et al.*, 2011), and soluble TNALP with the flag epitope at the C-terminus (TNALP-F) (Di Mauro *et al.*, 2002) were used as templates to generate the *Eco*RI-*Not*I fragments of three forms of TNALP cDNA by PCR cloning. Primers were designed to introduce an *Eco*RI or *Not*I recognition site at each end. These cDNA fragments were subcloned into the *Eco*RI and *Not*I sites of pcDNA (Invitrogen, San Diego, CA) AAV vector plasmid, pAAV.CAαGBE containing the CAG promoter and the globin polyadenylation signal (Takahashi *et al.*, 2002). AAV-GFP was used as a control AAV vector (Noro *et al.*, 2004). Recombinant AAV serotype 1 or 8 (AAV1 or AAV8) vectors were generated using the triple transfection method (Salvetti *et al.* 1998) and purified as described previously (Hermens *et al.*, 1999; Kurai *et al.*, 2007). The titer of each AAV vector was determined by real-time PCR (7500 Fast; Applied Biosystems, Tokyo, Japan).

Vector characterization

C2C12 cells were plated on 24-well plates at a density of 2×10^4 cells/well and transduced with three different AAV1-TNALP vectors [1.5×10^{11} vector genomes (vg)/well]. The medium was changed a day after transduction. Ninety-six hours after transduction, the transduced cells and the supernatants were separately collected and assayed for ALP activity.

Enzyme activity and protein assay

ALP activity was determined as previously described (Sogabe *et al.*, 2008). One unit was defined as the amount of enzyme needed to catalyze production of 1 μmol of *p*-nitrophenol per minute. ALP activity in plasma and cell culture supernatants was calculated as units per milliliter. Those of cells and organs were assayed with supernatants of homogenized cells and organs standardized by milligrams of protein. Protein concentration was assayed by the DC protein assay kit (Bio-Rad, Tokyo, Japan).

Mineralization assay

C2C12 cells were plated on six-well plates at a density of 4×10^4 cells/well and transduced with AAV1-TNALP-D10, AAV1-TNALP-F, or AAV1-GFP (control) vector. The medium was changed on the day after transduction. Seventy-two hours later, the cells were approximately 90–100% confluent, and the supernatants were collected for use in the mineralization assays. U2OS cells were plated on 96-well plates at a density of 1×10^4 cells/well and cultured for 48 hr to reach confluency. Their medium was then replaced with the conditioned medium from the C2C12 transductants. At the same time, 10 m*M* β-glycerophosphate (Sigma-Aldrich, St. Louis, MO) was added to verify the tendency for calcification. Five days after the medium change, cell calcification was evaluated as described previously (Johnson *et al.*, 2001; Orimo *et al.*, 2008).

Binding assay

ALP binding to hydroxyapatite (Sangi, Tokyo, Japan) was assayed as described previously with some modification (Nishioka *et al.*, 2006). Aliquots of each supernatant, adjusted based on ALP activity to 0.1 U/ml, were added to hydroxyapatite suspended in 25 m*M* Tris-buffered saline (TBS; 0.6 mg/500 μl) and incubated for 30 min at 37°C. Then the mixture was centrifuged to separate the unbound and bound enzyme. The difference in ALP activity was assayed before and after binding to hydroxyapatite. The percentage binding of the ALP activity was calculated as follows: % binding = [(ALP activity before binding) − (ALP activity after binding)]/(ALP activity before binding) ×100.

Inorganic pyrophosphate (PPi) assay

PPi of plasma was assayed as described previously (Lust and Seegmiller, 1976). Initially, protein in plasma was removed by centrifugation at 14,000 *g* for 25 min at 4°C with a Microcon-30 (Millipore, Bedford, MA). Thereafter, aliquots of the resultant solution were added to the wells of an OptiPlate-96 F black plate (PerkinElmer, Waltham, MA), and the fluorescent signals were read using a microplate reader (ARVO-MX 1420 multilabel counter; PerkinElmer) at 460 nm. Each sample was analyzed in triplicate.

Animal experiments

The generation and characterization of the *Akp2*$^{-/-}$ mice were described previously (Narisawa *et al.*, 1997). Genotyping was performed by PCR with primers 5′-AGTCCGTGG GCATTGTGACTA-3′ and 5′-TGCTGCTCCACTCACGTC GAT-3′. All animal experiments were performed according

to protocols approved by the Nippon Medical School Animal Ethics Committee. A 29-gauge insulin syringe was used to inject AAV8-TNALP and control AAV8-GFP vectors into the external jugular veins of 1-day-old mice (Ogawa *et al.*, 2009). Blood samples were collected from cut tails using heparinized capillaries on day 10 after birth and from the orbital sinus of anesthetized animals after day 14. We checked physical activity and healthy appearance together with the seizures in untreated ($n=9$), control AAV8-GFP–injected ($n=4$), and treated ($n=32$) mice every morning for about an hour per day for at least 1 month. During the observation periods, the behaviors as described on the Racine scale (Racine, 1972) were counted as convulsions. At 56 days of age, treated mice were sacrificed under deep anesthesia by perfusion with 20 ml of PBS containing 10 U/ml heparin, followed by an additional 20 ml of PBS to wash out the blood. Then the organs were harvested.

X-ray analysis

X-ray analysis was performed as previously described (Yamamoto *et al.*, 2011). In brief, radiographic images were obtained on μFX1000 film (Fujifilm Corp., Tokyo, Japan) that was set up for the analysis of small animals at an energy level of 25 kV and an exposure time of 90 sec for 10-day-old mice and 10 sec for 56-day-old mice.

Bone mineral density (BMD)

After skin and muscle were removed, the whole bones were stored in 75% ethanol until analysis. The right femur was dislocated and an X-ray image was taken to an IP plate using μFX1000 (Fujifilm Corp.), which is set up for the analysis of small animals. Each scan included a phantom (Kyoto Kagaku, Kyoto, Japan). This phantom contained six densities, from 0 to 100 mg/cm^2 by 20 mg/cm^2 K_2HPO_4; it was ordered to fit adult mice BMD. The BMD of each image was obtained (Typhoon FLA 7000; GE Healthcare Japan, Tokyo, Japan) with a personal computer and analyzed with Multi Gauge ver. 3.0 software (Fujifilm Corp.). BMD values were expressed in milligrams per square centimeter of K_2HPO_4. The region of interest for analysis was the whole femur.

Biodistribution of AAV vector

Genomic DNA was extracted from seven main organs (heart, lung, liver, spleen, kidney, muscle, bone) of AAV8-TNALP-D10–injected mice by using QIAamp DNA mini kit (QIAGEN, Valencia, CA). The DNA was subjected to real-time PCR to detect the copy number of AAV vector. In short, genome copy titers were quantified by TaqMan polymerase chain reaction (Applied Biosystems) using primers (forward: 5′-CGTCAATGGGTGGAGTATTTA-3′; reverse: 5′-AGGTCA TGTACTGGGCATAATGC-3′) and a probe designed against the cytomegalovirus primer. Genomic DNA spiked with AAV vector plasmid DNA was used as a standard, and average copy number per diploid was determined.

Histological examination

The bone was directly stained without fixation and decalcification. The knee joints were removed and embedded in SCEM compound (Leica Microsystems, Tokyo, Japan) without fixation. Sections (10 μm thick) were cut with the Kawamoto film method (Leica Microsystems) and washed with ethanol followed by dH_2O. ALP activity was assayed by incubating the tissue with 0.1 mg/ml naphthol AS-MX phosphate as a substrate and 0.6 mg/ml fast blue salt as dye in 20 ml of 0.1 *M* Tris-HCl buffer (pH 8.5) for approximately 15 min at 37°C, as described previously (Li *et al.*, 2007). The tissue sections were then mounted on silane-coated slides (Muto Pure Chemicals, Ltd., Tokyo, Japan) and examined under a light microscope (BX60; Olympus Ltd., Tokyo, Japan) (Sogabe *et al.*, 2008).

Statistical analysis

Data from *in vivo* and *in vitro* experiments are expressed as means ± SD. Differences between groups were tested for statistical significance using Student's *t* test. *P* values less than 0.05 were considered statistically significant. The survival rate was analyzed by the Kaplan–Meier method, and differences in the survival rates were assessed by the Wilcoxon test.

Results

Characterization of soluble TNALP in vitro

We generated AAV1 vectors expressing various forms of TNALP (Fig. 1A). After transduction of C2C12 cells with these vectors, the distribution of TNALP was examined. ALP activities from AAV1 vector containing TNALP-N were detected mainly in the cell lysate fraction (90.4 ± 1.4%), whereas the activities from AAV1 vectors with TNALP-F and TNALP-D10 were recovered only in the supernatant fraction (96.4 ± 0.4% and 96.6 ± 1.3%) ($n=4$ each). These results suggest that most of TNALP-N is anchored to the cell membrane like endogenous TNALP, and only a small portion (less than 10%) is solubilized by enzymatic cleavage. In contrast, TNALP-F and TNALP-D10 are synthesized as soluble enzymes. These soluble forms of TNALP were further characterized by an *in vitro* mineralization assay and binding assay.

In vitro *mineralization and affinity for hydroxyapatite*

To analyze the function and specificity of soluble forms of TNALP, we assessed its ability to mediate mineralization and to bind hydroxyapatite. Osteoblastic U2OS cells incubated with conditioned medium containing TNALP-F or TNALP-D10 were strongly stained by alizarin red S (0.83 ± 0.28 and 0.80 ± 0.49 U/mg protein vs. 0.26 ± 0.20 U/mg protein in mock control) (Fig. 1B). This strong staining indicates significantly accelerated mineralization.

The affinity of TNALP-F for hydroxyapatite mineral was studied by the *in vitro* binding assay. TNALP-D10 showed a stronger affinity to hydroxyapatite (88.3 ± 0.5 % bound) as compared with TNALP-F (13.9 ± 2.0 % bound), confirming the binding ability of deca-aspartate to hydroxyapatite described previously (Millán *et al.*, 2008) (Fig. 1C). The flag epitope has a stretch of four aspartates (Fig. 1A), but TNALP-F did not show any significant affinity to hydroxyapatite.

Sustained expression of TNALP-D10 and a prosurvival effect were detected in AAV8-TNALP-D10–treated mice

First, we evaluated the therapeutic efficacy of AAV-mediated expression of TNALP-D10 in *Akp2*$^{-/-}$ mice. We used

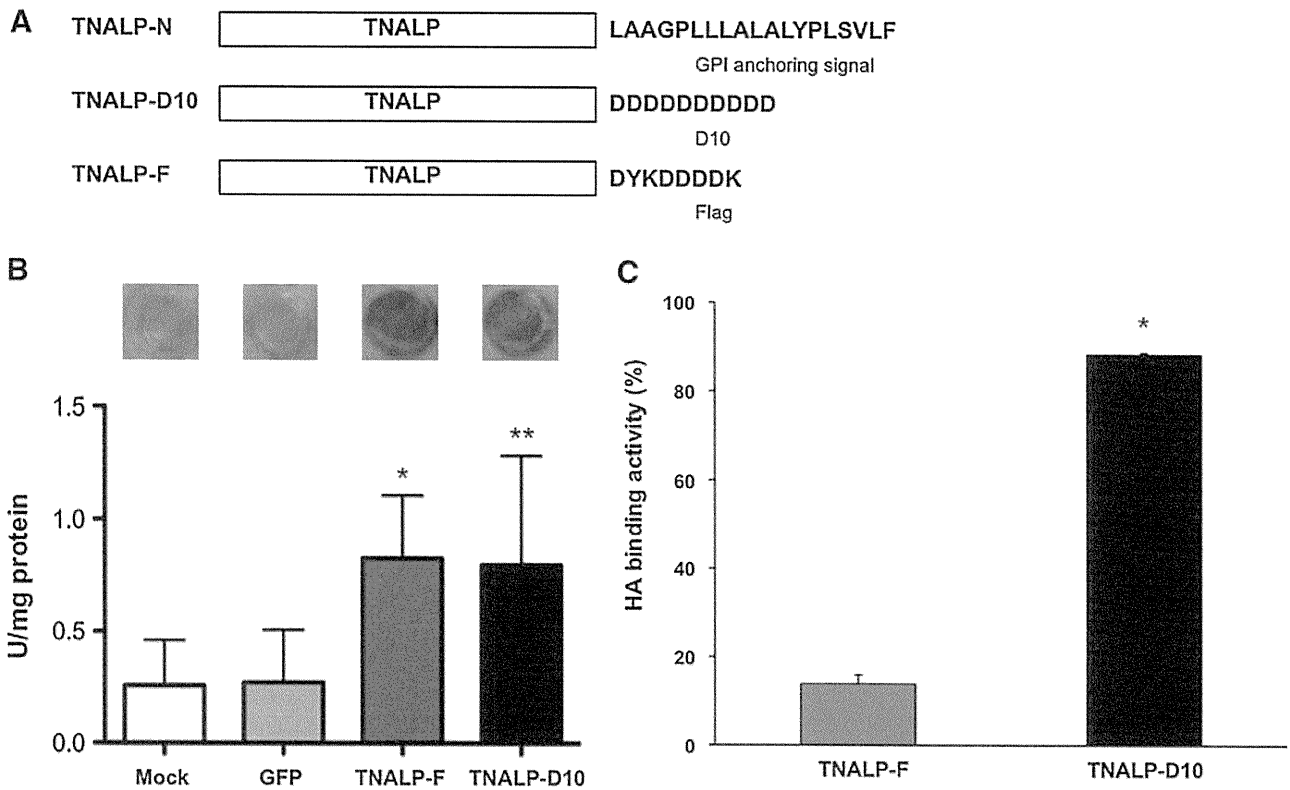

FIG. 1. Construction and characterization of TNALP. **(A)** Schematic representation of structure of native TNALP (TNALP-N), bone-targeted TNALP with D10 (TNALP-D10), and soluble TNALP with the flag epitope (TNALP-F). **(B)** *In vitro* mineralization assay. U2OS cells were incubated with the conditioned medium from C2C12 cells transduced with AAV1-TNALP-D10, AAV1-TNALP-F, or AAV1-GFP. Mock was analyzed without any vector. *Upper panel*: cell calcification stained with alizarin red S. *Lower panel*: quantitative analysis of cell calcification evaluated in cetylpyridinium chloride extraction by reading at 570 nm. $^{*}p < 0.005$, $^{**}p < 0.05$ as compared with the GFP-treated group. **(C)** *In vitro* binding assay. Hydroxyapatite was incubated with the conditioned medium from C2C12 cells transduced with AAV1-TNALP-F or AAV1-TNALP-D10. The percentage binding of TNALP was calculated by the difference in ALP activities before and after binding to hydroxyapatite. $^{*}p < 0.0001$ as compared with the TNALP-F group. HA, hydroxyapatite.

AAV8 vectors because the *in vivo* transduction efficiency of AAV8 is much higher than that of AAV1 (data not shown). AAV8-TNALP-D10 (5×10^{11} vg in 100 μl of PBS) was injected intravenously into the external jugular vein of 1-day-old *Akp2*$^{-/-}$ mice. The plasma ALP activity in these mice was markedly increased, and the superphysiologically high levels of ALP activity were sustained for at least 56 days (Fig. 2A). During this period, the mice appeared healthy. They had a normal physical activity level and no seizures, indicating that treatment by AAV-mediated gene therapy prevents *Akp2*$^{-/-}$ mice from having severe epileptic seizures. Two long-term follow-up survivors retained a high level of plasma ALP activity (9.0 ± 0.26 U/ml) and were healthy at more than 9 months after injection. Thus, a single injection of 5×10^{11} vg of AAV8-TNALP-D10 into *Akp2*$^{-/-}$ mice was sufficient for phenotypic correction and improved survival time.

TNALP dephosphorolates PPi, so that HPP patients show elevated plasma PPi concentrations, which inhibits hydroxyapatite crystal growth, leading to defective bone mineralization. Therefore, we next assayed plasma PPi levels in *Akp2*$^{-/-}$ mice. We found that, in untreated mice, plasma PPi levels were 30.0 ± 11.7 nmol/ml on day 10 after birth, but were only 24.5 ± 3.9 nmol/ml in mice administered AAV8-TNALP-D10, which is almost the same level as that in wild-type (WT) mice (25.0 ± 6.0 nmol/ml).

To determine the optimal dosage of AAV vector, we injected lower doses of AAV8-TNALP-D10 (5×10^{10} and 5×10^{9} vg/mouse) into 1-day-old *Akp2*$^{-/-}$ mice. Mice that received 5×10^{10} vg of AAV8-TNALP-D10 survived and appeared healthy, although their plasma ALP activity on day 28 was one order lower than that of mice that received 5×10^{11} vg (1.2 ± 0.7 U/ml vs. 13.7 ± 1.08 U/ml) (Fig. 2A). The mice that received the lowest dose (5×10^{9} vg) showed only a very slight increase in plasma ALP activity, and they died before weaning (similar to untreated *Akp2*$^{-/-}$ mice) (Fig. 2B). Thus, the optimal dosage of AAV8-TNALP-D10 to rescue the *Akp2*$^{-/-}$ mice was between 5×10^{10} and 5×10^{11} vg/mouse.

Therapeutic effects of TNALP-F and TNALP-N on survival

In the second series of animal experiments, we evaluated various forms of TNALP. *Akp2*$^{-/-}$ mice that received AAV8-TNALP-F (5×10^{10} vg/mouse) had a higher level of plasma ALP activity on day 28 than mice that received an equivalent dose of AAV8-TNALP-D10 (5.70 ± 2.57 U/ml vs. 1.20 ± 0.70 U/ml) (Fig. 3A). Seven of the nine mice that received

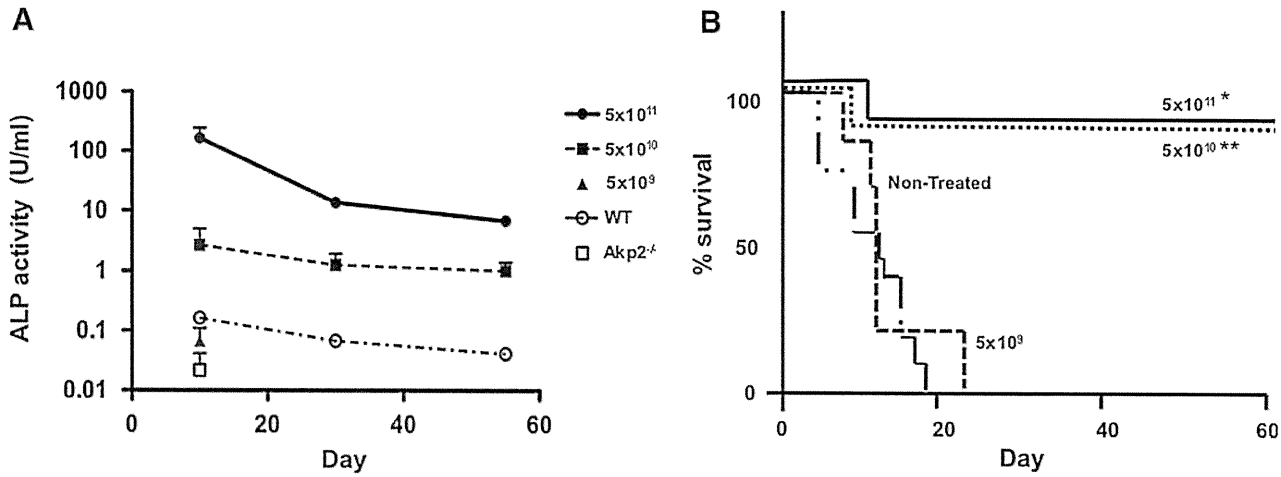

FIG. 2. Gene therapy of *Akp2*$^{-/-}$ mice with AAV8-TNALP-D10. Plasma ALP activity **(A)** and the survival curves **(B)** of *Akp2*$^{-/-}$ mice treated with AAV8-TNALP-D10 are shown. *Akp2*$^{-/-}$ neonatal mice were injected with 5×10^{11} ($n=7$), 5×10^{10} ($n=6$), and 5×10^{9} ($n=6$) vg/mouse doses of AAV8-TNALP-D10. Plasma ALP activities of treated mice, untreated *Akp2*$^{-/-}$ mice ($n=4$), and WT mice ($n=6$) were measured on days 10, 28, and 56 and are presented as the means×SD. The survival of mice was significantly prolonged by treatment with either 5×10^{11} or 5×10^{10} vg/mouse dose of AAV8-TNALP-D10. $^{*}p<0.001$, $^{**}p<0.003$ as compared with the nontreated group.

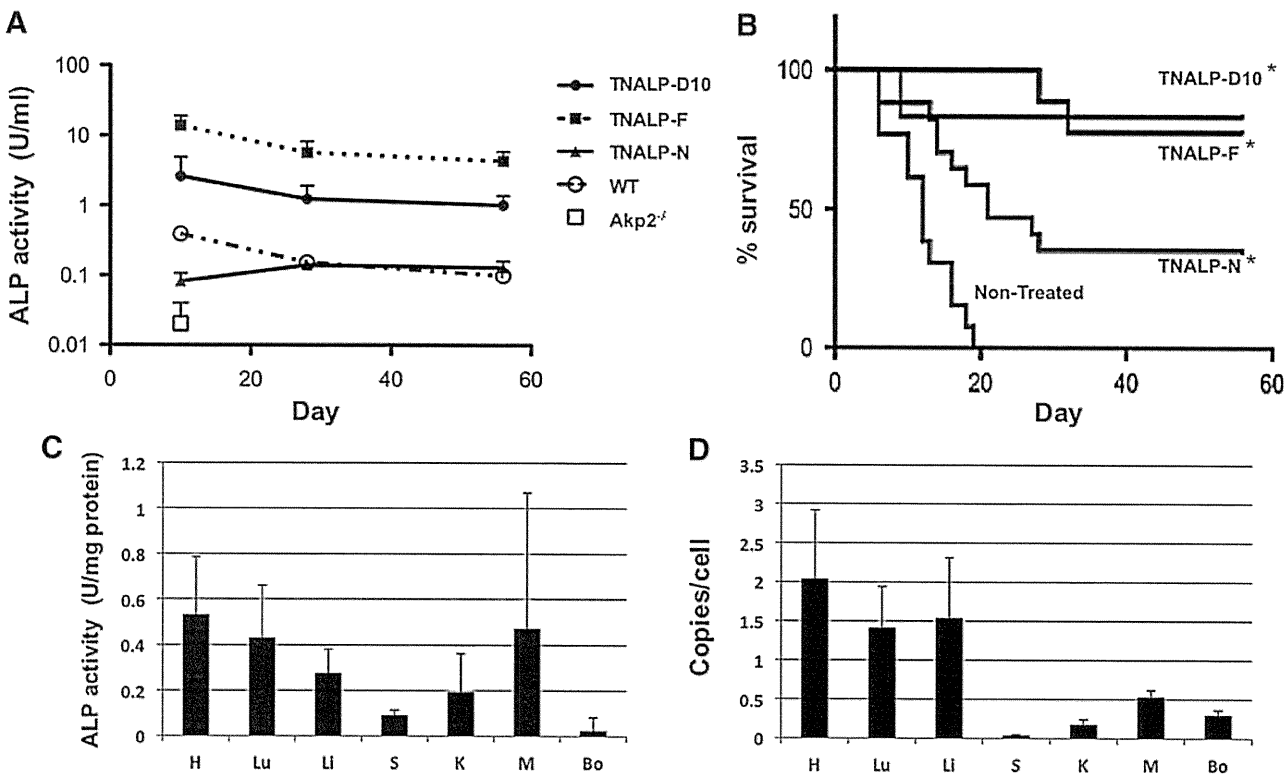

FIG. 3. Comparison of the therapeutic effects of AAV8-TNALP-D10, AAV8-TNALP-F, and AAV8-TNALP-N. Plasma ALP activity **(A)** and the survival curves **(B)** of *Akp2*$^{-/-}$ mice treated with 5×10^{10} vg/mouse doses of AAV8 vector expressing various forms of TNALP are shown. *Akp2*$^{-/-}$ neonatal mice were injected with AAV8-TNALP-D10 ($n=6$), AAV8-TNALP-F ($n=9$), or AAV8-TNALP-N ($n=17$). Plasma ALP activities of these treated mice, untreated *Akp2*$^{-/-}$ mice ($n=4$), and WT mice ($n=6$) were measured on days 10, 28, and 56 and are presented as the means×SD. The survival effects were observed in mice treated with AAV8-TNALP-D10, AAV8-TNALP-F, and AAV8-TNALP-N. $^{*}p<0.003$ as compared with the nontreated group. ALP activity **(C)** and vector distribution **(D)** in seven organs from AAV8-TNALP-N–injected **(C)** and AAV8-TNALP-D10–injected **(D)** *Akp2*$^{-/-}$ mice ($n=4$) are shown. H, heart; Lu, lung; Li, liver; S, spleen; K, kidney; M, muscle; Bo, bone.

AAV8-TNALP-F survived for at least 56 days (Fig. 3B). *Akp2*$^{-/-}$ mice that received AAV8-TNALP-N experienced a moderate increase in plasma ALP activity (0.14 ± 0.02 U/ml), indicating that some of the TNALP-N may have been solubilized by enzymatic cleavage, and five of the 17 mice in this group survived for at least 56 days (Fig. 3A and B). These results suggest that soluble TNALP, even without bone-targeted peptides, in the circulation shows favorable effects on prolongation of the lifespan of *Akp2*$^{-/-}$ mice.

To determine which organ(s) is the primary source of secreted TNALP in treated *Akp2*$^{-/-}$ mice, we investigated the ALP activity and vector distribution in seven organs from AAV8-TNALP-N– or D10–injected *Akp2*$^{-/-}$ mice. High ALP activities were detected in heart, skeletal muscle, lung, and liver (Fig. 3C). Real-time PCR analysis confirmed that these organs were efficiently transduced with AAV vector. Transduction of other organs, including bones, was very low (Fig. 3D).

Mature bone mineralization was detected in treated Akp2$^{-/-}$ *mice*

Bones in *Akp2*$^{-/-}$ mice treated with AAV vectors were evaluated by X-ray examination. *Akp2*$^{-/-}$ mice have a normal appearance at birth, but growth retardation and radiographic changes become apparent during the first 7 to 10 days of life. The severity of the mineralization defects is highly variable. One parameter for bone development is the timing of the appearance of secondary ossification centers (epiphyses) (Fedde *et al.*, 1999). Epiphyses in the knees of WT mice were well mineralized by day 10 (Fig. 4A). X-ray images of 10-day-old mice revealed that untreated and control AAV8-GFP–treated *Akp2*$^{-/-}$ mice did not have mineralized epiphyses, whereas apparent secondary ossification centers were detected in nine of 10 AAV8-TNALP-D10 (5×10^{11} vg)–treated mice. Mineralization of the epiphyses was also accelerated following AAV8-mediated expression of TNALP-D10. Untreated *Akp2*$^{-/-}$ mice died by day 20. After 56 days, epiphyses on the femurs and the tibias in treated *Akp2*$^{-/-}$ mice were well mineralized and became indistinguishable from those in WT mice (Fig. 4B). BMD showed no significant difference between treated *Akp2*$^{-/-}$ and WT mice (data not shown). These results indicate that a single injection of 5×10^{11} vg of AAV8-TNALP-D10 is effective in preventing the bone mineralization abnormalities and prolonging survival of *Akp2*$^{-/-}$ mice. We also examined the X-ray images of untreated ($n=11$) and AAV8-TNALP-D10 (5×10^{11} vg)–treated *Akp2*$^{-/-}$ mice ($n=9$) at day 10, and 56-day-old *Akp2*$^{-/-}$ mice successfully treated with various types of AAV8-TNALP (5×10^{10} vg, $n=32$). No apparent bone fractures were detected in both untreated and any of the surviving mice. In addition, mineralization of epiphyses at the forepaws and the knees was present in all surviving animals (Fig. 4B).

TNALP-D10 has high in vivo *affinity for bone*

A histological study of knee joints is illustrated in Fig. 5, in which fast blue staining indicates ALP activity. Neonatal injection of 5×10^{11} vg of AAV8-TNALP-D10 resulted in positive staining on the surface of the endosteal bone. No signals were detected in untreated *Akp2*$^{-/-}$ mice. Faint ALP staining occurred in mice that received 5×10^{10} vg of AAV8-TNALP-D10. *Akp2*$^{-/-}$ mice treated with 5×10^{10} vg of AAV8-TNALP-F and AAV8-TNALP-N showed no ALP-stained areas. These results confirm that TNALP-D10 has higher *in vivo* affinity for bone than TNALP-F.

Discussion

We previously demonstrated that the phenotypes of *Akp2*$^{-/-}$ mice can be corrected by continuous subcutaneous

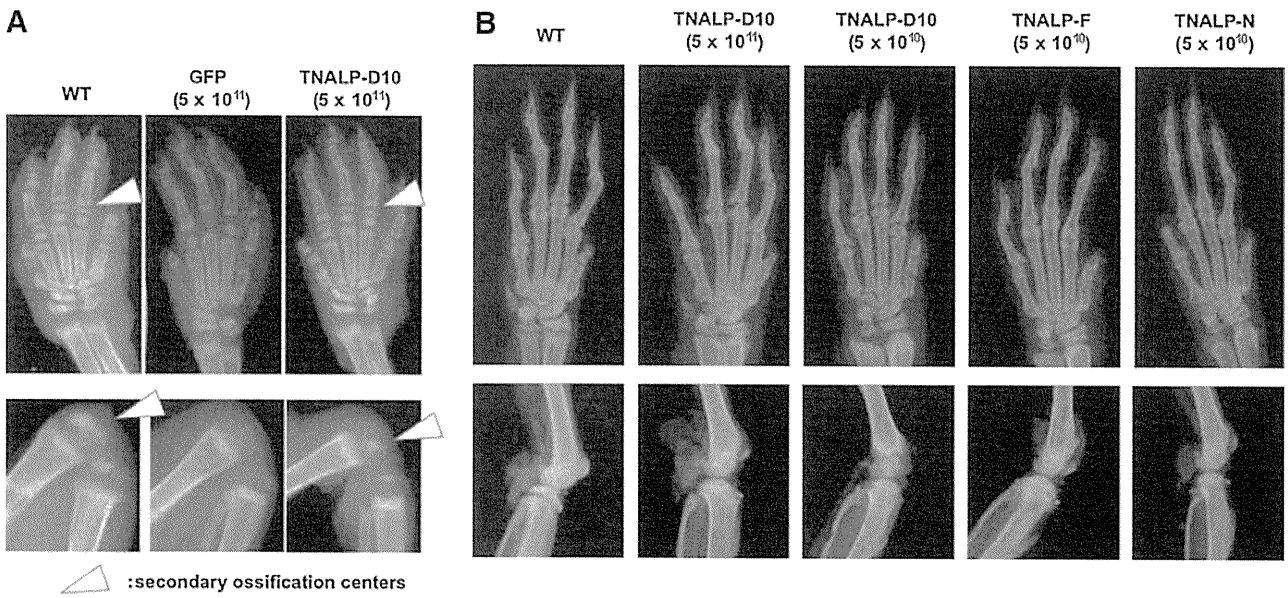

FIG. 4. X-ray images of knee joints and forepaws. **(A)** Secondary ossification centers in the femur, tibia, and digital bones were absent in the GFP-treated *Akp2*$^{-/-}$ mice (5×10^{11} vg/mouse), but were detectable in mice treated with AAV8-TNALP-D10 (5×10^{11} vg/mouse) on day 10. **(B)** Mineralization of epiphyses at the forepaws and the knee was shown in all surviving *Akp2*$^{-/-}$ mice treated with 5×10^{11} or 5×10^{10} vg/mouse doses of AAV8 vector expressing various forms of TNALP at 56 days of age.

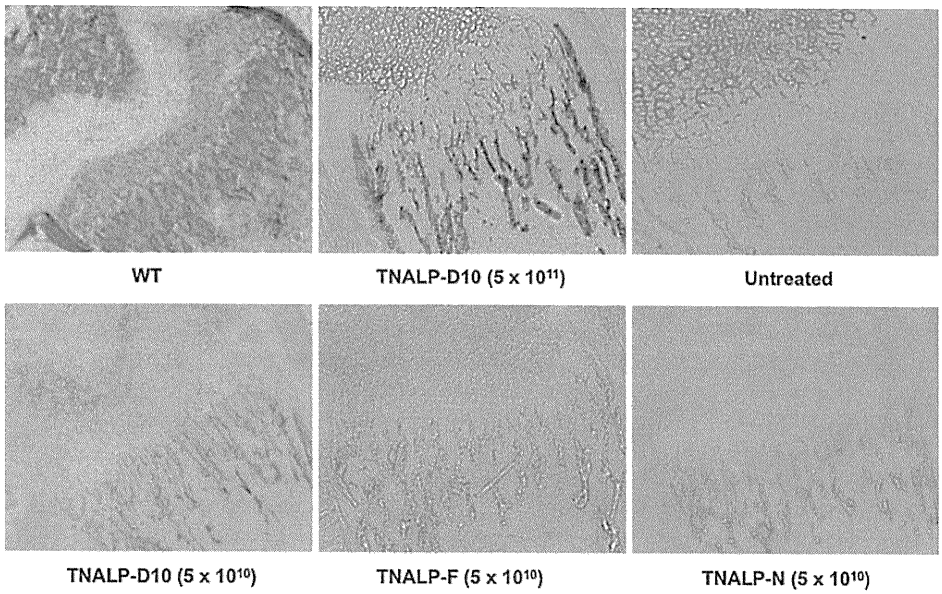

FIG. 5. Histochemical staining of ALP activity in the knee joints. ALP activity in the knee joints of *Akp2*$^{-/-}$ mice treated with various AAV vectors was directly stained with fast blue without fixation and decalcification at day 10. Blue staining was detected on the surface of the endosteal bone of WT mice and *Akp2*$^{-/-}$ mice treated with 5×10^{11} or 5×10^{10} vg/mouse doses of AAV8-TNALP-D10, but not of untreated *Akp2*$^{-/-}$ mice and *Akp2*$^{-/-}$ mice treated with 5×10^{10} vg/mouse doses of AAV8-TNALP-F and AAV8-TNALP-N. Original magnification, ×100.

injection or lentiviral-mediated expression of TNALP-D10 (Millán *et al.*, 2008; Yamamoto *et al.*, 2011). In the present study, we demonstrated that an intravenous injection of AAV8 vector expressing TNALP-D10 into neonatal *Akp2*$^{-/-}$ mice is also a highly effective treatment. These gene therapy approaches are minimally invasive, unlike classical ERT, which requires repeated injections of a large amount of enzyme (Millán *et al.*, 2008). Both lentiviral and AAV vectors worked efficiently to treat lethal HPP model mice. The high levels of ALP activity persisted for at least 9 months after a single injection of either vector in the neonatal period, but the time course of the plasma ALP activity was different between two vectors. When 5×10^{11} vg/mouse of AAV8-TNALP-D10 was injected, the plasma ALP level was initially extremely high (165.1 ± 79.8 U/ml on day 10), but decreased with time to a stable level (13.7 × 1.1 U/ml on day 28, 6.8 × 1.3 U/ml on day 56) (Fig. 2A). In contrast, ALP activities in plasma were relatively stable, ranging from 5.1 to 9.1 U/ml during 60 days after injection of 5×10^{7} TU/mouse HIV-TNALP-D10 (Yamamoto *et al.*, 2011). The rapid decline of ALP activity after AAV injection is thought to be due to a reduction of ALP expression in the liver. It was reported that AAV vector transduces the neonatal liver with high efficiency, but the expression is rapidly decreased mainly because episomal vector genomes are degraded in the liver at this developmental stage (Cunningham *et al.*, 2008; Inagaki *et al.*, 2008). There was no significant difference in bone mineralization between lentiviral- and AAV-treated mice. Integrating lentiviral vectors have been used for stable gene transfer into hematopoietic cells in *ex vivo* protocols (Cartier *et al.*, 2009; Kaiser, 2009), but their application for *in vivo* gene transfer is limited (Jarraya *et al.*, 2009). There is no clinical protocol for systemic lentiviral vector injection. In contrast, AAV vector is suitable for *in vivo* gene delivery and has been widely used for vector-mediated ERTs for genetic diseases, such as lysosomal storage disorders and hemophilia (Manno *et al.*, 2006; Kurai *et al.*, 2007; Passini *et al.*, 2007; Ogawa *et al.*, 2009). Taken together, both lentiviral and AAV vector are useful for treatment of HPP mice, but for clinical application, systemic delivery of AAV vector appears to be a more realistic approach to treat human patients.

An important finding is that soluble TNALP both with and without deca-aspartates is capable of rescuing lethal *Akp2*$^{-/-}$ mice when expressed by AAV vectors. A repeating sequence of acidic amino acids is found in several non-collagenous bone proteins and plays a key role in binding to bone (Kasugai *et al.*, 2000) and to hydroxyapatite (Nishioka *et al.*, 2006; Millán *et al.*, 2008). In an enzyme replacement approach, the use of TNALP with deca-aspartates, TNALP-D10, appears to be essential to treat HPP mice (Millán *et al.*, 2008). Previous human trials of ERT using various soluble ALP have shown very limited clinical and radiographic benefits (Whyte *et al.*, 1982, 1984, 1986; Weninger *et al.*, 1989). The main reason for these failures is thought to be the insufficient concentration of local ALP activity in skeletal tissues after systemic enzyme replacement. In contrast, TNALP-D10 has a high affinity for hydroxyapatite crystals and, therefore, ALP activity could be easily increased at the sites of skeletal mineralization. The efficacy of bone-targeted TNALP-D10 is now being evaluated in clinical trials of ERT.

In our gene therapy approach, the utility of deca-aspartates in the treatment of HPP model mice was not apparent. We confirmed that TNALP-D10 has a higher affinity for bone than TNALP-F both *in vitro* and *in vivo*. However, there was no significant difference in survival rate, convulsion frequency, and bone mineralization between mice treated with AAV8-TNALP-D10 and AAV8-TNALP-F. A potential advantage of AAV-mediated gene therapy compared with classical ERT is that a high concentration of soluble TNALP can be continuously supplied to systemic organs. Actually, very high levels of serum ALP activities were sustained in the circulation of both AAV8-TNALP-D10– and AAV8-TNALP-F–treated mice. The concentration of TNALP-F may be sufficient to keep the local ALP activity required for skeletal mineralization; even TNALP-F does not have a high affinity for bones. These data suggest that the use of soluble TNALP without additional peptides is an important option for treatment of HPP, at least in gene therapy approaches.

However, bone-targeted TNALP-D10 could be useful to reduce the vector dose and the safety concern in clinical gene therapy protocols. Further studies are required to optimize the vector construct for a safe and efficient gene therapy of HPP.

It was somewhat surprising that partial survival effects were also observed in animals treated with AAV8-TNALP-N. Synthesized TNALP-N is GPI-anchored to the cell membrane. A moderate increase in plasma ALP activity (around 0.1 U/ml) suggests that a portion of TNALP is released into the circulation by enzymatic cleavage. Only five of 17 *Akp2*$^{-/-}$ mice were rescued by neonatal injection of AAV8-TNALP-N, but surviving animals showed a healthy appearance and a normal activity with mature bone mineralization. These findings suggest that a circulating ALP activity level near 0.1 U/ml may be the threshold needed to inhibit seizures and prolong the survival of *Akp2*$^{-/-}$ mice, but sufficient to improve bone mineralization of surviving animals.

The major mechanism of gene therapy for HPP mice seems to be due to continuous supply of ALP activity from the circulation, but not genetic correction of bone cells. This speculation is strongly supported by the recent success of ERT of HPP (Millán *et al.*, 2008). Biodistribution of AAV vector demonstrated that major organs to secrete TNALP were heart and muscle. Transduction of bone tissues was very low. ALP staining in treated mice is due mainly to the circulating TNALP-D10 in the bone matrix. The contribution of *in situ* expression of TNALP in bone cells to bone mineralization is not likely to be significant. These data support the conclusion that normalizing systemic extracellular PPi concentrations is sufficient to prevent all the manifestations of HPP, in agreement with an earlier report describing correction of the HPP phenotype by the transgenic overexpression of GPI-anchored TNALP in the liver of *Akp2*$^{-/-}$ mice under the control of the apoprotein E promoter (Murshed *et al.*, 2005).

Pyridoxine-responsive seizures occur in some severe cases of human HPP, but they are not a common symptom (Mornet, 2007). The cause of these seizures is not completely understood, but they are thought to be due to reduced levels of pyridoxal 5′-phospate–dependent synthesis of the inhibitory neurotransmitter γ-aminobutyric acid in the brain (Waymire *et al.*, 1995; Narisawa *et al.*, 2001). The major clinical complications in human patients with HPP are directly related to defective skeletal mineralization (Whyte, 2002). Patients with severe infantile HPP usually die from respiratory failure caused by skeletal diseases in the chest, such as flail chest, rachitic deformity, and rib fractures (Whyte, 2002). Apnea is the major cause of death of *Akp2*$^{-/-}$ mice, but it appears to be caused by epileptic convulsions (not skeletal diseases) (Narisawa *et al.*, 1997).

It is unclear why skeletal disease is relatively mild in *Akp2*$^{-/-}$ mice, which have completely null TNALP activity. Other ALP isoenzymes or maternal TNALP may compensate for the virtual absence of endogenous TNALP. Indeed, recent findings have pointed to the nonredundant roles of PHOSPHO1 and TNALP in the initiation of endochondral ossification (Yadav *et al.*, 2011) and have also uncovered a potential compensating role of nucleoside triphosphate pyrophosphohydrolase-1 (NPP1) that might limit the severity of the TNALP null phenotype in *Akp2*$^{-/-}$ mice in the first days of life (Ciancaglini *et al.*, 2010; Yadav *et al.*, 2011). In the absence of TNALP, NPP1 has been found to act as the second best pyrophosphatase and ATPase in skeletal tissues (Ciancaglini *et al.*, 2010). Recent data indicate that skeletal mineralization is not affected in *Akp2*$^{-/-}$ mice due to the combined action of PHOSPHO1 and Pi-transporter-mediated influx of Pi into matrix vesicles (Ciancaglini *et al.*, 2010). Extravesicular propagation of hydroxyapatite deposition is impaired in *Akp2*$^{-/-}$ mice after postnatal day 6 due to the absence of TNALP's pyrophosphatase activity, but in the immediate postnatal state it has been argued that NPP1's pyrophosphatase activity can compensate for the lack of TNALP. Nevertheless, various degrees of mineralization defects are observed in untreated *Akp2*$^{-/-}$ mice after postnatal day 6. The delayed appearance of secondary ossification centers and carpal bones and the shortening of long bones are features of the neonatal period. A single injection of AAV8-TNALP-D10 prolonged survival and corrected the phenotype. Radiographic examination of these treated mice revealed accelerated mineralization of the epiphyses on day 10. No fractures were detected. Importantly, there were no significant differences in gross skeletal structure between mice treated with AAV8-TNALP-D10 and with AAV8-TNALP-F at 56 days of age. All surviving mice appeared healthy and had normal physical activity.

In conclusion, we successfully treated *Akp2*$^{-/-}$ mice with a single intravenous injection of AAV8 vector on day 1 after birth. Both bone-targeted TNALP-D10 and soluble TNALP were effective in inhibiting lethal seizures, prolonging survival, and improving bone mineralization. Thus, AAV8-mediated systemic gene therapy is a safe and effective treatment for the infantile form of HPP.

Acknowledgments

We thank Dr. James Wilson at the University of Pennsylvania for providing AAV packaging plasmids (p5E18RXC1 and p5E18-VD2/8). We thank Prof. Norio Amizuka at Hokkaido University and Prof. Kimimitsu Oda at Niigata University for their technical support of ALP activity staining. This work was supported in part by grants from the Ministry of Health, Labour and Welfare of Japan and the Ministry of Education, Culture, Sports, Science and Technology of Japan, by grant DE12889 from the National Institutes of Health USA, and by a grant from the Thrasher Research Fund.

Author Disclosure Statement

J.L. Millán is a consultant for Enobia Pharma, Inc. The other authors have no competing financial interests.

References

Cahill, R.A., Wenkert, D., Perlman, S.A., *et al.* (2007). Infantile hypophosphatasia: transplantation therapy trial using bone fragments and cultured osteoblasts. J. Clin. Endocrinol. Metab. 92, 2923–2930.

Camacho, P.M., Painter, S., and Kadanoff, R. (2008). Treatment of adult hypophosphatasia with teriparatide. Endocr. Pract. 14, 204–208.

Cartier, N., Hacein-Bey-Abina, S., Bartholomae, C.C., *et al.* (2009). Hematopoietic stem cell gene therapy with a lentiviral vector in X-linked adrenoleukodystrophy. Science 326, 818–823.

Ciancaglini, P., Yadav, M.C., Simao, A.M., *et al.* (2010). Kinetic analysis of substrate utilization by native and TNAP-,

NPP1-, or PHOSPHO1-deficient matrix vesicles. J. Bone Miner. Res. 25, 716–723.

Cunningham, S.C., Dane, A.P., Spinoulas, A., *et al.* (2008). Gene delivery to the juvenile mouse liver using AAV2/8 vectors. Mol. Ther. 16, 1081–1088.

Di Mauro, S., Manes, T., Hessle, L., *et al.* (2002). Kinetic characterization of hypophosphatasia mutations with physiological substrates. J. Bone Miner. Res. 17, 1383–1391.

Fedde, K.N., Blair, L., Silverstein, J., *et al.* (1999). Alkaline phosphatase knock-out mice recapitulate the metabolic and skeletal defects of infantile hypophosphatasia. J. Bone Miner. Res. 14, 2015–2026.

Goseki-Sone, M., Orimo, H., Iimura, T., *et al.* (1998). Expression of the mutant (1735T-DEL) tissue-nonspecific alkaline phosphatase gene from hypophosphatasia patients. J. Bone Miner. Res. 13, 1827–1834.

Hermens, W.T., Ter Brake, O., Dijkhuizen, P.A., *et al.* (1999). Purification of recombinant adeno-associated virus by iodixanol gradient ultracentrifugation allows rapid and reproducible preparation of vector stocks for gene transfer in the nervous system. Hum. Gene Ther. 10, 1885–1891.

Inagaki, K., Piao, C., Kotchey, N.M., *et al.* (2008). Frequency and spectrum of genomic integration of recombinant adeno-associated virus serotype 8 vector in neonatal mouse liver. J. Virol. 82, 9513–9524.

Jarraya, B., Boulet, S., Ralph, G.S., *et al.* (2009). Dopamine gene therapy for Parkinson's disease in a nonhuman primate without associated dyskinesia. Sci. Transl. Med. 1, 2ra4.

Johnson, K., Hashimoto, S., Lotz, M., *et al.* (2001). Up-regulated expression of the phosphodiesterase nucleotide pyrophosphatase family member PC-1 is a marker and pathogenic factor for knee meniscal cartilage matrix calcification. Arthritis Rheum. 44, 1071–1081.

Kaiser, J. (2009). Gene therapy. Beta-thalassemia treatment succeeds, with a caveat. Science 326, 1468–1469.

Kasugai, S., Fujisawa, R., Waki, Y., *et al.* (2000). Selective drug delivery system to bone: small peptide $(Asp)_6$ conjugation. J. Bone Miner. Res. 15, 936–943.

Kurai, T., Hisayasu, S., Kitagawa, R., *et al.* (2007). AAV1 mediated co-expression of formylglycine-generating enzyme and arylsulfatase A efficiently corrects sulfatide storage in a mouse model of metachromatic leukodystrophy. Mol. Ther. 15, 38–43.

Li, M., Sasaki, T., Ono, K., *et al.* (2007). Distribution of macrophages, osteoclasts and the B-lymphocyte lineage in osteolytic metastasis of mouse mammary carcinoma. Biomed. Res. 28, 127–137.

Lust, G., and Seegmiller, J.E. (1976). A rapid, enzymatic assay for measurement of inorganic pyrophosphate in biological samples. Clin. Chim. Acta 66, 241–249.

Manno, C.S., Pierce, G.F., Arruda, V.R., *et al.* (2006). Successful transduction of liver in hemophilia by AAV-Factor IX and limitations imposed by the host immune response. Nat. Med. 12, 342–347.

Millán, J.L. (2006). *Mammalian Alkaline Phosphatases. From Biology to Applications in Medicine and Biotechnology.* (Wiley-VCH, Weinheim, Germany).

Millán, J.L., Narisawa, S., Lemire, I., *et al.* (2008). Enzyme replacement therapy for murine hypophosphatasia. J. Bone Miner. Res. 23, 777–787.

Mornet, E. (2007). Hypophosphatasia. Orphanet. J. Rare Dis. 2, 40.

Murshed, M., Harmey, D., Millán, J.L., *et al.* (2005). Unique coexpression in osteoblasts of broadly expressed genes accounts for the spatial restriction of ECM mineralization to bone. Genes Dev. 19, 1093–1104.

Narisawa, S., Frohlander, N., and Millán, J.L. (1997). Inactivation of two mouse alkaline phosphatase genes and establishment of a model of infantile hypophosphatasia. Dev. Dyn. 208, 432–446.

Narisawa, S., Wennberg, C., and Millán, J.L. (2001). Abnormal vitamin B6 metabolism in alkaline phosphatase knock-out mice causes multiple abnormalities, but not the impaired bone mineralization. J. Pathol. 193, 125–133.

Nishioka, T., Tomatsu, S., Gutierrez, M.A., *et al.* (2006). Enhancement of drug delivery to bone: characterization of human tissue-nonspecific alkaline phosphatase tagged with an acidic oligopeptide. Mol. Genet. Metab. 88, 244–255.

Noro, T., Miyake, K., Suzuki-Miyake, N., *et al.* (2004). Adeno-associated viral vector-mediated expression of endostatin inhibits tumor growth and metastasis in an orthotropic pancreatic cancer model in hamsters. Cancer Res. 64, 7486–7490.

Ogawa, K., Hirai, Y., Ishizaki, M., *et al.* (2009). Long-term inhibition of glycosphingolipid accumulation in Fabry model mice by a single systemic injection of AAV1 vector in the neonatal period. Mol. Genet. Metab. 96, 91–96.

Orimo, H., Goseki-Sone, M., Hosoi, T., and Shimada, T. (2008). Functional assay of the mutant tissue-nonspecific alkaline phosphatase gene using U2OS osteoblast-like cells. Mol. Genet. Metab. 94, 375–381.

Passini, M.A., Bu, J., Fidler, J.A., *et al.* (2007). Combination brain and systemic injections of AAV provide maximal functional and survival benefits in the Niemann-Pick mouse. Proc. Natl. Acad. Sci. U.S.A. 104, 9505–9510.

Racine, R.J. (1972). Modification of seizure activity by electrical stimulation. II. Motor seizure. Electroencephalogr. Clin. Neurophysiol. 32, 281–294.

Salvetti, A., Oreve, S., Chadeuf, G., *et al.* (1998). Factors influencing recombinant adeno-associated virus production. Hum. Gene Ther. 9, 695–706.

Sogabe, N., Oda, K., Nakamura, H., *et al.* (2008). Molecular effects of the tissue-nonspecific alkaline phosphatase gene polymorphism (787T>C) associated with bone mineral density. Biomed. Res. 29, 213–219.

Tadokoro, M., Kanai, R., Taketani, T., *et al.* (2009). New bone formation by allogeneic mesenchymal stem cell transplantation in a patient with perinatal hypophosphatasia. J. Pediatr. 154, 924–930.

Takahashi, H., Hirai, Y., Migita, M., *et al.* (2002). Long-term systemic therapy of Fabry disease in a knockout mouse by adeno-associated virus-mediated muscle-directed gene transfer. Proc. Natl. Acad. Sci. U.S.A. 99, 13777–13782.

Waymire, K.G., Mahuren, J.D., Jaje, J.M., *et al.* (1995). Mice lacking tissue non-specific alkaline phosphatase die from seizures due to defective metabolism of vitamin B-6. Nat. Genet. 11, 45–51.

Weninger, M., Stinson, R.A., Plenk, H. Jr., *et al.* (1989). Biochemical and morphological effects of human hepatic alkaline phosphatase in a neonate with hypophosphatasia. Acta Paediatr. Scand. Suppl. 360, 154–160.

Whyte, M.P. (2002). Hypophosphataia. In *The Metabolic and Molecular Bases of Inherited Deseases.* C.R. Scriver, A.L. Beaudet, W.S. Sly, *et al.*, eds. (McGraw-Hill, New York, NY) pp. 5319–5329.

Whyte, M.P., Valdes, R. Jr., Ryan, L.M., and McAlister, W.H. (1982). Infantile hypophosphatasia: enzyme replacement therapy by intravenous infusion of alkaline phosphatase-rich plasma from patients with Paget bone disease. J. Pediatr. 101, 379–386.

Whyte, M.P., McAlister, W.H., Patton, L.S., *et al.* (1984). Enzyme replacement therapy for infantile hypophosphatasia attempted by intravenous infusions of alkaline phosphatase-rich Paget plasma: results in three additional patients. J. Pediatr. 105, 926–933.

Whyte, M.P., Magill, H.L., Fallon, M.D., and Herrod, H.G. (1986). Infantile hypophosphatasia: normalization of circulating bone alkaline phosphatase activity followed by skeletal remineralization. Evidence for an intact structural gene for tissue nonspecific alkaline phosphatase. J. Pediatr. 108, 82–88.

Whyte, M.P., Kurtzberg, J., McAlister, W.H., *et al.* (2003). Marrow cell transplantation for infantile hypophosphatasia. J. Bone Miner. Res. 18, 624–636.

Whyte, M.P., Mumm, S., and Deal, C. (2007). Adult hypophosphatasia treated with teriparatide. J. Clin. Endocrinol. Metab. 92, 1203–1208.

Yadav, M.C., Simao, A.M., Narisawa, S., *et al.* (2011). Loss of skeletal mineralization by the simultaneous ablation of PHOSPHO1 and alkaline phosphatase function: a unified model of the mechanisms of initiation of skeletal calcification. J. Bone Miner. Res. 26, 286–297.

Yamamoto, S., Orimo, H., Matsumoto, T., *et al.* (2011). Prolonged survival and phenotypic correction of Akp2$^{-/-}$ hypophosphatasia mice by lentiviral gene therapy. J. Bone Miner. Res. 26, 135–142.

Address correspondence to:
Dr. Takashi Shimada
Department of Biochemistry and Molecular Biology
Nippon Medical School
1-1-5 Sendagi, Bunkyo-ku
Tokyo 113-8602
Japan

E-mail: tshimada@nms.ac.jp

Received for publication November 1, 2010;
accepted after revision March 10, 2011.

Published online: March 10, 2011.

ORIGINAL ARTICLE

JBMR

Prolonged Survival and Phenotypic Correction of *Akp2*$^{-/-}$ Hypophosphatasia Mice by Lentiviral Gene Therapy

Seiko Yamamoto,[1,2] Hideo Orimo,[1] Tae Matsumoto,[1] Osamu Iijima,[1] Sonoko Narisawa,[3] Takahide Maeda,[2] José Luis Millán,[3] and Takashi Shimada[1]

[1]Department of Biochemistry and Molecular Biology, Nippon Medical School, Tokyo, Japan
[2]Department of Pediatric Dentistry, Nihon University Graduate School of Dentistry at Matsudo, Matsudo, Japan
[3]Sanford-Burnham Medical Research Institute, La Jolla, CA, USA

ABSTRACT

Hypophosphatasia (HPP) is an inherited systemic skeletal disease caused by mutations in the gene encoding the tissue-nonspecific alkaline phosphatase (*TNALP*) isozyme. The clinical severity of HPP varies widely, with symptoms including rickets and osteomalacia. *TNALP* knockout (*Akp2*$^{-/-}$) mice phenotypically mimic the severe infantile form of HPP; that is, *TNALP*-deficient mice are born with a normal appearance but die by 20 days of age owing to growth failure, hypomineralization, and epileptic seizures. In this study, a lentiviral vector expressing a bone-targeted form of *TNALP* was injected into the jugular vein of newborn *Akp2*$^{-/-}$ mice. We found that alkaline phosphatase activity in the plasma of treated *Akp2*$^{-/-}$ mice increased and remained at high levels throughout the life of the animals. The treated *Akp2*$^{-/-}$ mice survived for more than 10 months and demonstrated normal physical activity and a healthy appearance. Epileptic seizures were completely inhibited in the treated *Akp2*$^{-/-}$ mice, and X-ray examination of the skeleton showed that mineralization was significantly improved by the gene therapy. These results show that severe infantile HPP in *TNALP* knockout mice can be treated with a single injection of lentiviral vector during the neonatal period. © 2011 American Society for Bone and Mineral Research.

KEY WORDS: ALKALINE PHOSPHATASE; LENTIVIRAL VECTOR; ENZYME REPLACEMENT; EPILEPSY; CALCIFICATION

Introduction

Hypophosphatasia (HPP) is an inherited skeletal disease caused by mutations in the gene encoding the tissue-nonspecific alkaline phosphatase (*TNALP*) isozyme.[1] The symptoms of HPP include hypomineralization that causes rickets in infants and children and osteomalacia in adults.[2,3] The clinical severity of HPP varies widely from a lethal perinatal form to mild odontohypophosphatasia that manifests only dental abnormalities.[4] In the infantile form, postnatal development appears to proceed normally before the onset of failure to thrive and the associated development of rickets before 6 months of age. Severe infantile HPP is often fatal.[3]

TNALP is an ectoenzyme that is attached to the outer plasma membrane via a glycosylphosphatidylinositol (GPI) anchor.[5,6] Absence of TNALP activity results in extracellular accumulation of natural substrates such as inorganic pyrophosphate (PP_i),[7,8] pyridoxal 5′-phosphate (PLP),[9,10] and phosphoethanolamine (PEA).[11] Since high concentrations of PP_i result in a strong inhibition of hydroxylapatite crystal growth, normal mineralization of the systemic bones and teeth is impaired in HPP patients.[8,12] Pyridoxine-responsive seizures are also observed in some severe cases. Enzyme-replacement therapy using various types of alkaline phosphatase[13–17] and cell therapy using bone marrow cells[18,19] and mesenchymal cells[20] have been reported with no or very limited clinical benefit.

TNALP knockout mice have been established in two independent laboratories.[21,22] These mice are born with a normal appearance but, owing to deficient degradation of PP_i and abnormal metabolism of PLP, develop rickets and die by 20 days of age as a result of severe skeletal hypomineralization and epileptic seizures and represent an appropriate model of the infantile form of HPP.[23,24] Recently, Millán and colleagues[25] treated *TNALP* knockout mice with a daily subcutaneous injection of a bone-targeted form of TNALP in which a bone-targeting deca-aspartate sequence was linked to the C-terminal end of soluble TNALP.[26,27] Based on those data, clinical trials of enzyme-replacement therapy with bone-targeted TNALP in

Received in original form December 31, 2009; revised form June 5, 2010; accepted July 22, 2010. Published online August 4, 2010.
Address correspondence to: Takashi Shimada, MD, PhD, Department of Biochemistry and Molecular Biology, Nippon Medical School, 1-1-5 Sendagi, Bunkyo-ku, Tokyo 113-8602, Japan. E-mail: tshimada@nms.ac.jp

Journal of Bone and Mineral Research, Vol. 26, No. 1, January 2011, pp 135–142
DOI: 10.1002/jbmr.201

patients with adult and infantile HPP have been initiated.[28] A limitation of enzyme-replacement therapy for HPP is the restricted half-life of the TNALP protein in patients' fluids and tissues, which necessitates repeated administration of large amounts of the enzyme for long-term correction.

In this study, we examined viral vector–mediated gene therapy of HPP. We found that a single injection of lentiviral vector expressing bone-targeted TNALP into neonatal HPP mice resulted in long-term high levels of ALP in the serum and long-term phenotypic correction in HPP mice. We conclude that gene therapy may prove to be an important option for the treatment of human HPP.

Materials and Methods

Plasmid construction

To create *TNALP-D10* cDNA coding for TNALP lacking the GPI anchor sequence and containing 10 repeated aspartic acid (Asp) residues at its C-terminus, polymerase chain reaction (PCR) was performed using primers *TNALP-D10*-f (5′-GAA TTC ACC CAC GTC GAT TGC ATC TCT CTG GGC TCC AG) and *TNALP-D10*-r (5′-GAA TTC TCA GTC GTC ATC ATC ATC ATC GTC GTC ATC GTC GTC GCC TGC GGA GCT GGC AGG AGC ACA GTG-3′) with pcDNA3 *TNALP* cDNA plasmid as the template.[29] The PCR product then was digested with *Eco*RI and inserted into the pGEM T-easy vector (Promega Corporation, Madison, WI, USA). A second PCR was performed using primers *Eco*RI–*TNALP*-f (5′-TTT GAA TTC GCC ACC ATG ATT TCA CCA TTC TTA GTA C-3′) and *TNALP-D10-Not*I-r (5′-TTT GCG GCC GCT CAG TCG TCA TCA TCA TCA TCG). The orientation of each sequence then was confirmed.

The pHIV-TNALP-D10 plasmid was constructed by insertion of the *Eco*RI and *Not*I fragments containing the cDNA for *TNALP-D10* into pC1(–)3UTR-del, which is a newly constructed SJ1-based HIV-1 vector containing 0.25-kb insulators in the U3 and the murine stem cell virus (MSCV) long terminal repeat (LTR) as an internal promoter (Fig. 1*A*).[30]

Lentiviral vector preparation

Lentiviral vector was prepared by transient transfection in 293T cells, as described previously.[30] Vector preparation treated with Benzonase (50 μL/mL) for 1 hour at room temperature was filtrated by 0.45-μm membrane after adjustment of the pH to 8.0 with 1 N NaOH. Vector was concentrated using Acrodisc Units with Mustang Q Membranes (PALL Corporation, Ann Arbor, MI, USA).[31,32] The eluted solution containing lentiviral vector was ultracentrifuged with a 20% (w/v) sucrose underlay for purification, and the infectious vector particle (titer) was determined in HeLa cells. The titer was expressed as transducing units per milliliter (TU/mL).

Animal procedures and experiments

All animal experiments were preapproved by the Nippon Medical School Animal Ethics Committee. Wild-type (WT) $Akp2^{+/+}$ heterozygous (HET) and $Akp2^{-/-}$ knockout (HPP) mice were obtained by mating $Akp2^{+/-}$ heterozygous mice with mice of a mixed 129J × C57Bl/6J genetic background.[22] Lentiviral vector (5.0×10^7 TU/100 μL in PBS) was injected into the jugular vein of neonatal mice on days 1 through 3. Breeding HET pairs were fed modified Laboratory Rodent Diet 5001 (Purina Mills, St Louis, MO, USA)[35] composed of CMF laboratory feed (Oriental Yeast Co., Ltd., Tokyo, Japan) supplemented with 325 ppm pyridoxine/10 kg of feed.

ALP activity

Blood samples were collected from the tail vein or the orbital sinus. The level of ALP in the plasma was quantified using a colorimetric assay for ALP activity, as described previously.[36] ALP activity was determined using 10 mM *p*-nitrophenyl phosphate (Sigma-Aldrich, Steinheim, UK) as the substrate in 100 mM 2-amino-2-methyl-1,3-propanediol-HCl buffer containing 5 mM $MgCl_2$ (pH 10.0) at 37°C. ALP enzyme activity was described in units (U) defined as the amount of enzyme needed to catalyze production of 1 μmol of *p*-nitrophenol formed per minute. ALP activity in plasma was calculated as units per milliliter (U/mL).

Biodistribution of lentiviral vector

Mice were deepley anesthesized and perfused with 15 mL of PBS containing 150 U of heparin and 15 mL of PBS. The liver, spleen, kidney, lung, heart, and bone (femur) were harvested, and homogenates were made using the Percellys-24 bead-beating homogenizer according to the company's protocol (Bertin Technologies, Paris, France). Genomic DNA was extracted from tissue homogenates using the Gentra Puregene Kit (Qiagen Siences, Germantown, MD, USA) and was subjected to real-time PCR to estimate the distribution. The primer/probe sets FPLV2 (modified at one base to 5′-ACT TGA AAG CGA AAG GGA AAC-3′ owing to a difference in the HIV-1 strain), RPLV2 (5′-CAC CCA TCT CTC TCC TTC TAG CC-3′), and LV2 (5′-AGC TCT CTC GAC GCA GGA CTC GGC -3′) were used to detect the lentiviral vector provirus, as described previously.[33] TaqMan ribosomal RNA control reagents (Applied Biosystems, Branchburg, NJ, USA) were used to quantify the amount of genomic DNA. To estimate vector distribution, genomic DNA extracted from the bone marrow cells of BL/6 wild-type mice or genomic DNA spiked with plasmid DNA was used as a standard, and average copy number per diploid were determined.[34]

X-ray analysis

Digital microradiography images were obtained using a μFX-1000 (Fujifilm, Tokyo, Japan) and imaged with FLA-7000 (Fujifilm). The X-ray energy levels were 25 kV and 100 μA, and an exposure time of 90 seconds was used for 15-day-old mice, and 15 seconds was used for adult mice. We examined a minimum of three X-ray pictures from each group at given ages.

ALP activity staining

Bone samples were fixed in neutral buffered formalin for 24 hours at 4°C. Knuckle samples then were decalcified in 10% EDTA solution with rotation for 2 to 3 days at 4°C. For the azo-dye method, knuckles were embedded in optimal-cutting-temperature (OCT) compound (Tissue-Tek, SAKUSA Finetechnical, Tokyo, Japan) and sectioned using a Leica CM1950 cryostat. Thin sections (4 μm thick) were air-dried for 10 minutes, washed in

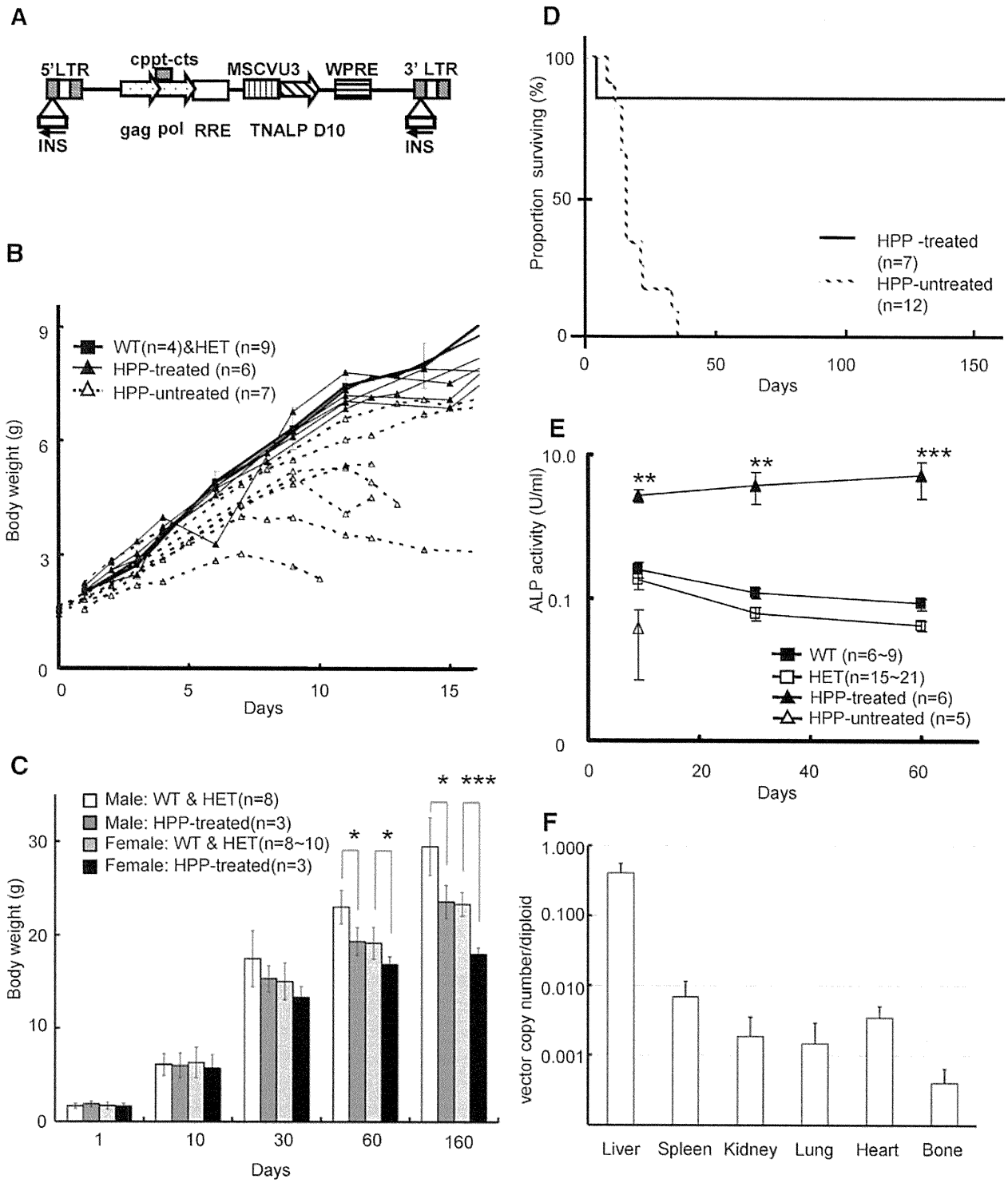

Fig. 1. Lentiviral-mediated gene therapy of *Akp2*$^{-/-}$ hypophosphatasic (HPP) mice. (*A*) Schematic diagram of HIV-TNALP-D10 lentiviral vector. LTR = long terminal repeat; MSCVU3 = U3 region of the LTR promoter of murine stem cell virus; WPRE = woodchuck hepatitis virus posttranscriptional regulatory element; INS = chicken β-globin hypersensitivity site 4 insulator; cppt-cts = central polypurine tract–central termination sequence; RRE = reverse responsive element. (*B*) Growth curves of untreated HPP mice ($n = 7$), treated HPP mice ($n = 6$), and WT ($n = 4$) and HET ($n = 9$) mice. The body weights of untreated HPP mice were recorded until spontaneous death. The weights of WT and HET (total $n = 13$) mice are presented as the average ± SD. (*C*) The comparison of average body weights of treated HPP mice (male, $n = 3$; female, $n = 3$) and WT/HET littermates (male, $n = 8$; female, $n = 8$ to 10). $^{*}p < .05$; $^{***}p < .001$. (*D*) The survival curves of treated ($n = 7$) and untreated ($n = 12$) HPP mice. (*E*) Concentration of plasma ALP in the treated ($n = 6$) and untreated ($n = 5$) HPP mice and HET ($n = 15$ to 21) and WT ($n = 6$-9) controls. $^{**}p < .01$ versus the WT group; $^{***}p < .001$ versus the WT group. (*F*) Distribution of lentiviral vector. The copy numbers of the vector genome in the organs was determined by qPCR with HIV-TNALP-D10 injected WT mice. Data are presented as mean ± SEM ($n = 4$).